Asian Journal of Chemistry; Vol. 27, No. 5 (2015), 1857-1860

ASIAN JOURNAL OF CHEMISTRY

http://dx.doi.org/10.14233/ajchem.2015.18222

Study on Hydrothermal Synthesis and Characterization of Ce-Y/SBA-15 Composite Materials

CHUNWEI SHI[1,2], WENYUAN WU[1,*], XUE BIAN[1], XIN WANG[3], JIANHONG LI[2], SHANLIN ZHAO[2], PING CHEN[2], YUTING BAI[1] and WEIYA YANG[3]

[1]Liaoning Shihua University, Fushun 113001, Liaoning Province, P.R. China
[2]School of Materials and Metallurgy, Northeastern University, Shenyang 110819, Liaoning Province, P.R. China
[3]Sinopec Fushun Research Institute of Petroleum and Petrochemicals, Fushun 113001, Liaoning Province, P.R. China

*Corresponding author: Tel: +86 24 83680527; E-mail: wuwynu@163.com

Received: 30 May 2014; *Accepted*: 11 August 2014; *Published online*: 20 February 2015; AJC-16906

Cerium iron was successfully incorporated into an Y/SBA-15 micro-mesoporous molecular sieve *via* the hydrothermal synthesis method. A series of characterizations were used to characterize the prepared materials such as XRD, N_2-adsorption-desorption, SEM-EDS and TEM. The results showed that the prepared composite materials kept the highly ordered mesoporous two-dimension hexagonal structure of SBA-15 and octagonal structure of Y, while the preparation of Ce-Y/SBA-15 composite materials has the advantages of high plentiful cerium iron (2.30 % wt). In the prepared Ce-Y/SBA-15, the frameworks were kept intact, their structures were still kept high ordered and the cerium iron locates inside the pores of Y/SBA-15.

Keywords: Micro-mesoporous composite materials, Modified molecular sieve, Cerium, Catalysis.

INTRODUCTION

Micro-mesoporous composite materials are distributed in double models of microporous structure and mesoporous structure, with a moderate ratio of microporous to mesoporous[1,2] and combines the advantages of mesoporous materials, *i.e.*, highly-ordered structure and adjustable pore size[3,4]; and advantages of microporous materials, *i.e.*, strong activation cenetr and high thermal & hydrothermal stability. Thus, the microporous and messporous structures can complement each other's advantages and realize a synergistic effect[5]. Furthermore, the mesoporous materials with large pore sizes can provide a channel for the macromolecular catalytic reactions, while the pore structures with fully crystallized or partially crystallized hold walls can benefit the micromolecular shape-selective catalysis or macromolecular catalytic reactions requiring strong acid sites[6,7].

In order to improve the surface acidity of micro-mesoporous composite materials, both organic and inorganic methods have been used in the modification of the micro-mesoporous composite materials, in order to improve the surface acidity of it, such as the application of SnO-SBA-15 prepared *via* incipient-wetness impregnation method in ester exchange reactions[8]. In recent years, the incorporation of heteroatoms into the mesoporous molecular sieve has aroused a great deal of interest. Due to their high electric densities, the transition metals and rare earth metal ions, can be loaded in the molecular sieve, which will further remarkably increase the acid sites of the molecular sieve and its catalytic activity after incorporated into mesoporous materials[9]. Duan *et al.*[10] reported the effect of cerium doped micro-mesoporous on the complete catalytic oxidation of benzene and they found that the existence of mesoporous will exert a negatiev influence on the catalyst activity of cerium doped Co_3O_4/ZSM-5 microporous sieve. Shi *et al.*[11] investigated that the addition of cerium can effectively promote the catalytic oxidation activity of Pd/HZSM-5 micro-mesoporous composite material for methane. Choi *et al.*[12] reported that hierarchical zeolite ZSM-5 was successfully synthesized by adding organosilane surfactant as templates. The catalytic results of molecular sieve showed that, hierarchical zeolite molecular sieve was superior to conventional ZSM-5 zeolites on the aspect of catalytic performance in catalytic reactions involving macromolecular compounds. Wang *et al.*[13] applied modified composite materials in hydrocracking by taking MCM-41/Y composite molecular sieve and amorphous silica-alumina as main acid components added with W-Ni active metal components.

In the present paper, we studied the modification effect of Ce on Ce-Y/SBA-15. The Ce modified Y/SBA-15 composite material was characterized by using powder X-ray diraction (XRD), low-temperature N_2 adsorption techniques, SEM/EDS, TEM, *etc*.

EXPERIMENTAL

Sodium aluminate, sodium hydroxide, sodium silicate and tetraethyl orthosilicate (TEOS) were all analytical pure reagents and purchased from Sinopharm Group Co. Ltd. Triblock copolymer poly(ethylene glycol)-block-poly(propylene glycol)-block-poly(ethylene glycol) (Pluronic P123) was purchased from Sigma Aldrich, America.

Hydrothermal synthesis of microporous material Y

Preparation of directing agent: 2.05 g sodium aluminate was dissolved in 45 mL deionized water followed by the addition of 10.45 g sodium hydroxide. To the mixture of above solution was added 27 mL sodium silicates, stirred for 15 min and then heated up in water bath at 65 °C. After 0.5 min, the resulting solution was suddenly quenched to afford the directing agent, with the following molar ratio of $16Na_2O:Al_2O_3:15SiO_2:320H_2O$.

Preparation of mother liquid: 2.05 g sodium aluminate was dissolved in 25 mL deionized water followed by the addition of 0.3 g sodium hydroxide. The mixture of above solution was slowly added with 3 mL directing agent and 17 mL sodium silicate, then stirred for 20 min to afford a mixture with the following molar ratio of $4.3Na_2O:Al_2O_3:10SiO_2:180\ H_2O$. The mother liquid was crystalized in hydrothermal reaction kettle at 100 °C for 19 h, the mixture was extracted and filtrated several times and the resultant solid was washed with 30 mL ethanol and then dried to afford Y-type zeolite molecular sieve.

Hydrothermal synthesis of mesoporous material SBA-15[14]

Hydrothermal synthesis of micro- and mesoporous composite materials: 4 g triblock copolymer poly(ethylene glycol)-block-poly(propylene glycol)-block-poly (ethylene glycol) P123 was dissolved in 30 g of deionized water and stirred until fully dissolved. To the above solution was added 9.5 g of tetraethyl orthosilicate (TEOS) and stirred magnetically and powerfully, followed by the addition of 2 g prepared Y type microporous materials and 120 mL certain conc. HCl, resulting a mixture solution with pH of 2 by a powerful magnetic stirring. After reacting in hydrothermal reaction kettle at 100 °C for 24 h, the crystallized product was washed with fresh deionized water and transferred again in an autoclave dried at 110 °C. Finally, the solid was calcined at 550 °C to afford a powder micro-mesoporous Y/SBA-15 composite material.

Synthesis of cerium modified micro-mesoporous composite material: Certain amount of cerium nitrate was dissolved in concentrated sulfuric acid to afford a saturated $Ce(NO_3)_2$-H_2SO_4 solution, followed by the addition of the activated Y/SBA-15. 1 g of the calcined Y/SBA-15 composite material was impregnated with 15 mL saturated $Ce(NO_3)_2$-H_2SO_4 solution and stirred at room temperature for 24 h. The resulting mixture was filtrated several times and the resultant solid was transferred again in an autoclave dried at 100 °C for 24 h. Finally, the solid was calcined at 550 °C for 3 h to afford the desired catalyst.

Catalyst characterization: The nitrogen adsorption and desorption method was employed to analyze the specific surface area and pore size of the sample. Sample was measured at a constant temperature of 77.35 K, with a equilibrium time of every 10 s. The pore size was measured in the range of 1.7-80 nm.

X-ray powder diffraction data was obtained on D/Max-2500 diffractometer using CuK_α 1 radiation ($\lambda = 15.4056$ nm) operated at 40 KV and 80 mA. The test pace and scanning rate of SXRD were 0.01° and 2°/min, respectively, in the range of 0.4-8°. While the test pace and scanning rate of WXRD were 0.1° and 8°/min, respectively, in the range of 10-70°.

Scanning electron microscopy (SEM/EDS) images were recorded on a JEOL JSM-7500F SEM instrument. Transmission electron microscopy (TEM) images were taken on JEM-2100 instrument at an acceleration voltage of 200 kV. The samples were sonicated in A.R. grade ethanol for 15 min and the resulting suspension was allowed to dry on carbon film supported on copper grids.

RESULTS AND DISCUSSION

X-ray powder diffraction: Fig. 1a showed the powder small angle XRD patterns (SXRD) of SBA-15, Y/SBA-15 and Ce modified Y/SBA-15; while Fig. 1b described the powder wide-angle X-ray scattering spectra of Y, Y/SBA-15 and Ce modified Y/SBA-15.

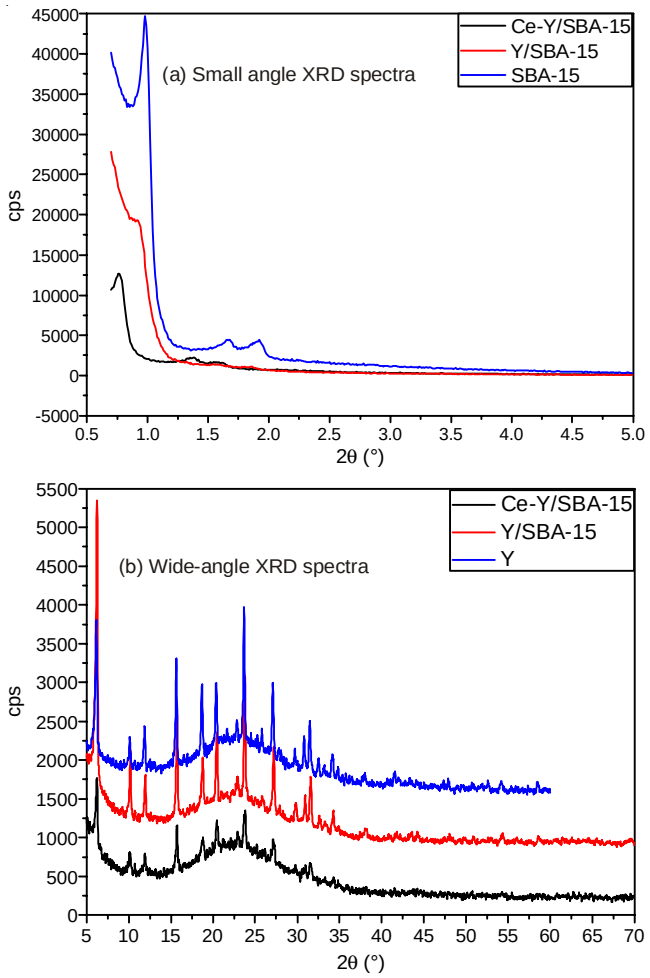

Fig. 1. XRD spectra of Y, SBA-15, Y/SBA-15 and Ce-Y/SBA-15

As shown in Fig. 1a, three reflection peaks (100), (110) and (200) of samples' small-angle characteristic diffraction peaks were resolved and could be indexed in the hexagonal space group, which indicated a highly ordered hexagonal mesoporous structure of prepared SBA-15. The characteristic

peak of Y/SBA-15 was decreased and it could be inferred that the introduction of Y type zeolite molecular sieve into the framework of mesoporous materials could lower the amount of pure crystallized mesoporous molecular sieves. However, the modified Y/SBA-15 peak moving to higher angles indicated that Ce species might be incorporated into the framework of molecular seive. All three peaks d (100), d (110) and d (200) of the sample moved to lower angles obviously, which implied the existence of SBA-15 framework in both composite materials and modified composite materials.

Fig. 1b described the difference between the WXRD curve of Y/SBA-15 and that of Y and SBA.-15. Besides, the WXRD curve of Y/SBA-15 was not a simple addition of Y and SBA-15, which indicated that micro-mesoporous Y/SBA-15 composite material synthesized by hydrothermal treatment could not be achieved by mechanical mixing of Y and SBA-15. In the wide angle range of 10-70°, all three samples possessed Y type characteristic peaks, while the addition of SBA-15 dramatically decreased the intensity of Y peak and its crystallinity. Furthermore, cerium modified Y/SBA-15 possessed a weaker Y peak intensity and lower crystallinity.

N_2 adsorption-desorption analysis: Fig. 2 showed the adsorption-desorption isotherms of Y, SBA-15, Y/SBA-15 and cerium modified Y/SBA-15 materials.

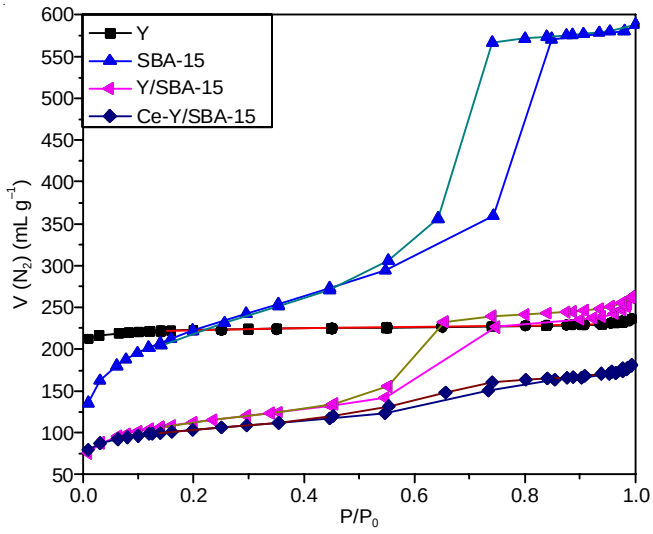

Fig. 2. N_2 adsorption and desorption isotherms of four samples

It could be seen from Fig. 3 that the adsorption-desorption isotherm of Y belonged to type I, curves of typical microporous molecular sieve type, while that of SBA-15 was in type IV referred as curves of typical mesoporous molecular sieve type. Y/SBA-15 and modified Y/SBA-15 showed the typical type IV curves at relative low pressure stage; when $P/P_0 < 0.1$, the adsorption and desorption curves were completely overlapped and the absorption amount significantly increased along with increase of P/P; when $0.1 < P/P_0 < 0.35$, the adsorption amount increased along with the increase of P/P_0, with a lower increase of N_2 adsorption compared with that in the stage of $P/P_0 < 0.1$, which was attributed to the monolayer dispersion of N_2 at the inner surface of mesoporous materials at a low differential pressure. Under a relatively low to medium pressure, the adsorption curve rised when $P/P_0 > 0.35$ as the relative pressure increased, due to capillary condensation of N_2 within mesoporous materials formed by the skeletons. The mesoporous material was fully filled of capillary condensed N_2, which caused the remakable increase of absorption amount and the jump of adsorption curve consistent with P/P_0 although the surface area of cerium modified Y/SBA-15 decreased, the N_2 low temperature adsorption-desorption isotherms of the sample still kept its specific type IV abdorption-desorption isotherms which only slightly shifted to the low pressure area. Thus, it indicated that, the introduction of Ce to Y/SBA-15 molecular sieves caused the partial contraction of mesporous channel.

The pore size distribution curves of three samples were shown in Fig. 3. As shown in Fig. 3, the pore sizes of SBA-15, Y/SBA-15 and Ce-Y/SBA-15 were 6.36 nm, 6.13 and 5.69 nm, respectively, which indicated that the introduction of Y and Ce to SBA-15 molecular sieves caused the partial contraction of mesporous pore size.

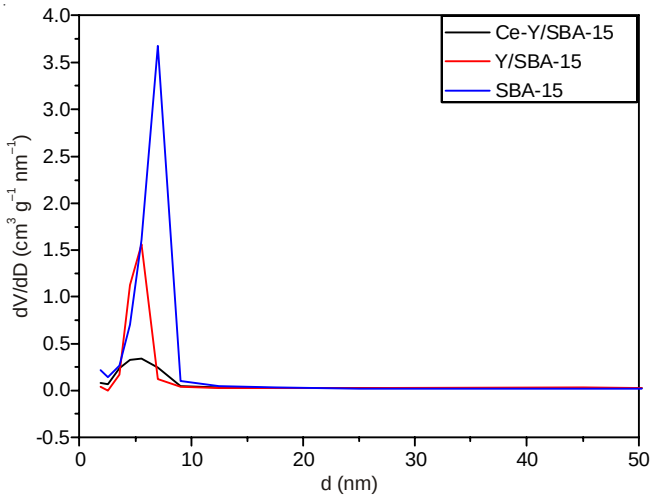

Fig. 3. Pore size distribution of three samples

SEM/EDS elemental analysis: Fig. 4 showed the SEM/EDS pictures of the modification of Y/SBA-15 by rare-earth Ce.

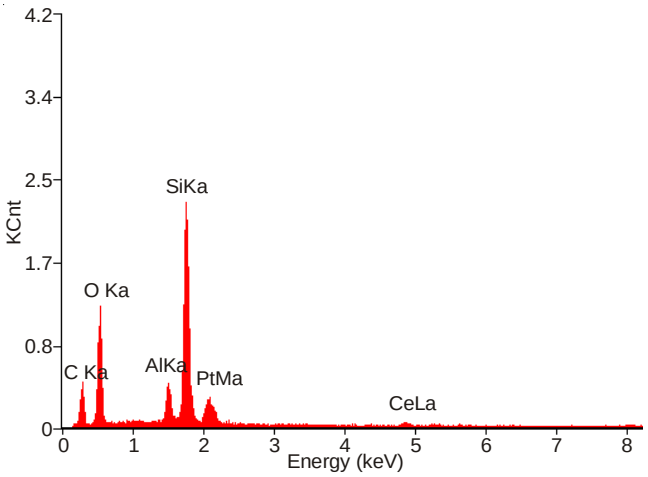

Fig. 4. SEM/EDS pictures of the modification of micro-mesoporous molecular sieve by cerium

Table-1 comprises the result of element analysis by SEM/EDS.

TABLE-1
RESULT OF ELEMENT ANALYSIS BY SEM/EDS

Catalyst	w (Elements) (%)					
	Si	Al	Ce	O	C	Pt
Y/SBA-15	22.97	3.97	0	41.47	21.92	9.67
Ce-Y/SBA-15	18.41	3.13	2.30	35.68	31.49	8.99

It could be seen from Fig. 4 that, the cerium element appeared in X-ray spectrum peaks of the SEM/EDS pictures. As shown in Table-1, the mass of Ce content was 2.30 %, Si/Al molar ratios from 6.78 to 6.88. Cerium which replaced Al impregnated into the composite zeolite framework. Cerium changed Si/Al molar ratios of the compound zeolite, there by changed its structure and catalytic properties.

Transmission electron microscopy: Fig. 5 showed TEM micrographs of Y/SBA-15 and Ce-Y/SBA-15.

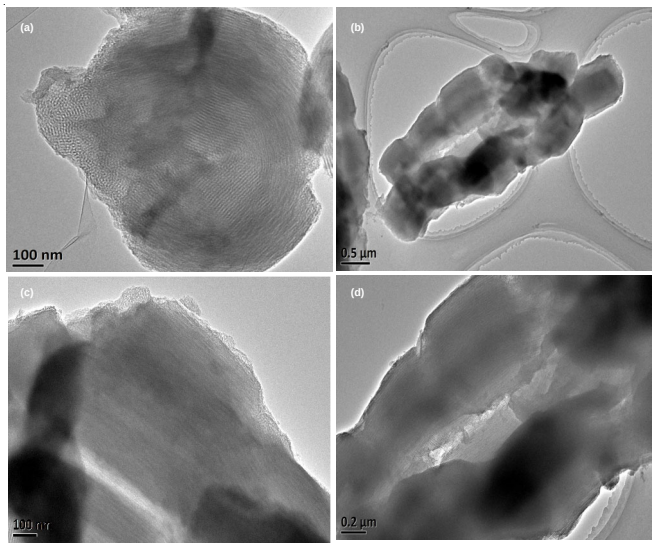

Fig. 5. TEM photos of Y/SBA-15 (a) (b) and Ce-Y/SBA-15 (c) (d)

The junction of microporous and mesoporous can be seen in TEM photos. Y was the core and SBA-15 wrapped on the outside. The overall shape of compound zeolite was similar to the lotus. TEM images show that the highly ordered micro-mesoporous structures of the Y/SBA-15 remain after the formation of Ce^{4+} inside the Y/SBA-15 channels. Moreover, small clusters encapsulated inside the micro-mesoporous channels can also be discerned and no large particles located outside the mesopores are observed.

Conclusions

• The combination of a series of characterization techniques has demonstrated that Ce can be doped inside the pores of the micro-mesoporous Y/SBA-15 molecular sieve with 2.30 % (wt). The results showed that the frameworks of the prepared Ce-Y/SBA-15 composite materials were intact, the micro-mesoscopic ordering degrees were still very high and were kept high ordered.

• Due to the existence of micro-mesoporous composite channel structure in the catalyst, the entry of Ce^{4+} to the channel dramatically increases the active centers, thus the catalytic activity of the catalyst is enhanced correspondingly. Future work will be focused on the study of structure characteristics of Ce-Y/SBA-15 materials.

REFERENCES

1. F.J. Shiring, R. Venkatadri and J.G. Goodwin Jr, *Can. J. Chem. Eng*., **61**, 218 (1983).
2. L.P. Liu, G. Xiong, X.S. Wang, J. Cai and Z. Zhao, *Micropor. Mesopor. Mater*., **123**, 221 (2009).
3. Y.H. Ma, H.L. Zhao, S.J. Tang, J. Hu and H.-L. Liu, *Acta Phys. Chim. Sin*., **27**, 689 (2011).
4. Z.Y. Feng, X.W. Huang, H.J. Liu, M. Wang, Z.Q. Long, Y. Yu and C. Wang, *J. Rare Earths*, **30**, 903 (2012).
5. W.Y. Wu and X. Bian, The Technology of Rare Earths Metallurgy, Science Press, Beijing (2012).
6. X.H. Vu, N. Steinfeldt, U. Armbruster and A. Martin, *Micropor. Mesopor. Mater*., **164**, 120 (2012).
7. Y.-Y. Li, B. Yan, L. Guo and Y.-J. Li, *Micropor. Mesopor. Mater*., **148**, 73 (2012).
8. P. Shah, A.V. Ramaswamy, K. Lazar and V. Ramaswamy, *Appl. Catal. A*, **273**, 239 (2004).
9. O. Olkhovyk, S. Pikus and M. Jaroniec, *J. Mater. Chem*., **15**, 1517 (2005).
10. Y.P. Zheng, S.R. Wang, Z.R. Wang, L.W. Wu and Y.M. Sun, *J. Rare Earths*, **28**, 92 (2010).
11. C. Shi, L. Yang and J. Cai, *Fuel*, **86**, 106 (2007).
12. M. Choi, H.S. Cho, R. Srivastava, C. Venkatesan, D.-H. Choi and R. Ryoo, *Nat. Mater*., **5**, 718 (2006).
13. D.Q. Wang, F.M. Sun and P.F. Jia, *Refining Technol. Eng*., **43**, 45 (2013).
14. D.Y. Zhao, J.L. Feng, Q.S. Huo, N. Melosh, G.H. Fredrickson, B.F. Chmelka and G.D. Stucky, *Science*, **279**, 548 (1998).